# Experimental Investigation of Two-Phase Flow Patterns in a Vertical to Horizontal Bend Pipe Using Wire-Mesh Sensor

**LOKMAN A. ABDULKAREEM[1,2]\*, VEYAN A. MUSA[3], RAID A. MAHMOOD[3,4], EZIDEEN A. HASSO[5]**

[1] Institute of Fluid Dynamics, Helmholtz-Zentrum Dresden-Rossendorf, Bautzner Landstr 400, Dresden 01328, Germany
[2] Department of Petroleum Engineering, University of Zakho, Zakho City, P.O. Box 12, Northern Iraq
[3] Department of Mechanical Engineering, University of Zakho, Zakho city, P.O. Box 12, Northern Iraq
[4] School of Mechanical and Electrical Engineering, University of Southern Queensland, Australia
[5] Department of Energy, College of Engineering, Dohuk Polytechnic University, Dohuk, Northern Iraq

*Abstract: The air-water two-phase flow plays an important role in many applications of industry fields. Usually, a 90-degree bend is used to connect pipes for changing the direction of flow which influences the two-phase flow pattern. In this paper, the effect of 90-degree bend under different ranges of gas and liquid superficial velocities on the two-phase flow patterns in the horizontal pipe located after the bend was experimentally investigated, and then results were presented and compared in a two-phase flow pattern map. Also, tomographic images and probability density functions were used to capture the cross-section void fraction and its distribution for the two-phase flow patterns. The results revealed that at low liquid and gas flow rates, a stratified-wavy flow pattern was observed as a dominant flow pattern. While the wavy-annular and semiannular flow patterns were observed at a high range of gas flow rates in the horizontal pipe. The results also showed that at the high range of liquid flow rate, bubbly, plug, slug, stratified-wavy, and wavy-annular flow patterns were observed in the horizontal pipe when the gas flow increased. The tomographic images and probability density functions gave good agreement with the experimental observations and results.*

*Keywords: air-water flow in pipes, two-phase flow in bends, wire Mesh Sensor (WMS)*

## 1. Introduction

The air-water two-phase flow exists in many mechanical and chemical applications such as that in transportation pipelines and power generation stations, it also plays an important role in other scientific fields, such as physics, biology, and meteorology [1]. The behavior of two-phase flow in elbows and bends presents an intractable challenge due to the geometrical structure and unpredictable distribution when the flow passes through the elbows and bends under the impact of centrifugal, gravitational, and buoyancy forces, therefore; the two-phase flow patterns must be considered to enhance the efficiency of flow process system [2]. Much attention has been given by previous studies to investigate the two-phase flow behavior and its pattern in elbows and bents pipes. Dean [3] investigated the effect of the different curvature's radius of the bent tubes on the flow behavior, the study proposed the Dean number (Dn) as a function of Reynolds number (Re), a diameter of the tube (Dpipe), and curvature's radius of the bend (Rcurv).

Gardner and Neller [4] studied the air-water two-phase flow behavior in a 90-degree bend with an internal diameter of 76 mm. The study investigated the impact of bend angular (φ) and the influence of increasing the superficial velocities on the two-phase flow behavior. The results presented the relationship between the centrifugal and gravity force in a correlation and dimensionless parameter called Froude number (Fr). The results also reported three configurations of the flow: homogeneous flow when the Fr is equal to one, the gas phase moves to the external axial side of the curve and the liquid phase tends to flow in the internal axial side when the Fr is less than one, finally, the gas tends to move to the internal axial side of the bend when the Fr is greater than one. Taitel and Dukler [5] reported a mathematical equation to identify the two - phase flow patterns in bends. The study proposed that the

---

*\*email: lokman.abdulkareem@uoz.edu.krd.*

annular flow pattern occurred when the ratio between the liquid height and pipe diameter is equal or less than 0.5. The results also revealed that the transition between the stratified and slug flow patterns is depending on the liquid height (h) which started from the pipe base. Usui et al. [6] presented a theoretical study to investigate the void fraction ($\alpha$) of the two-phase flow in a bend when the flow direction changed from horizontal to vertical. The results presented a correlation for dimensionless parameters between the centrifugal and gravitational forces to represent the Froude number for different two-phase flow patterns. Kim et al. [7] presented an experimental study to investigate the two-phase flow patterns for the air-water flow in a 90-degree elbow of an internal diameter of 50.3 mm. The results revealed that the angle of the elbow influenced the two-phase flow patterns and has a significant effect on flow behavior. The bubbly flow regime in a developed region in a horizontal pipe after the elbow was observed in the experiments.

Abdulkadir et al. [8] presented an experimental study using the Wire-Mesh Sensor (WMS) as a tomographic image sensor to investigate the two-phase flow patterns of air-silicone oil flow in a vertical pipe through a bend to a horizontal pipe of internal diameter 67 mm and a curvature radius of 154 mm. The results revealed that the bend with a 154 mm curvature radius has a significant effect on the two-phase flow pattern. Annular, stratified wavy, slug, plug, and annular flow patterns in the horizontal pipe directly after the bend were observed in the experiments. Salve et al [9] investigated the two-phase flow patterns experimentally using the Wire-Mesh Sensor (WMS). Air-water two-phase flow was the forking fluid in a horizontal pipe of internal diameter 19.5 mm and an aggregate length of 6 m. The results revealed that the stratified, plug, slug, and annular flow regimes were identified using the Probability Density Function (PDF) technique. Liu et al. [10] presented an experimental study using Wire mesh sensor (WMS) to capture the two-phase flow patterns of air-water flow in a horizontal pipe of 50 mm internal diameter, the probability density function (PDF) technique and a void fraction ($\alpha$) of time series were used to improve the results. The results presented different flow patterns such as Stratified, Wavy, Annular flow, plug, and slug flow regimes at different values of superficial velocities.

Kong et al [11] investigated the two-phase flow patterns for air-water flow in a horizontal pipe with an internal diameter of 38 mm. The study assessed the behavior of the two-phase flow at a different range of superficial velocities for the air and water phases. The study also considered the transition between the two-phase flow patterns such as the bubbly, plug, and slug pattern. The results revealed that the bubbles flow at the upper part of the pipe at a low liquid flow rate and then the bubbles start to coalesce to create large bubbles. While the plug flow regime generated when the flow rate of liquid decreased further. Besana and Mazza [12] investigated the effect of a 90-degree bend with an internal diameter of 26 mm and with a curvature radius of 143 mm on the air-water two-phase flow patterns. A high-speed camera was used to record the two-phase flow behavior. The study presented the slug flow through a vertical pipe which represents the upstream flow after a horizontal pipe which represents the downstream. Abdulkadir [13] presented an intensive study to estimate the two-phase flow patterns of gas-silicone oil flow in a blend under different range of gas superficial velocity (Usg) and liquid superficial velocity (Usl). Wire mesh sensor was used to predict the two-phase flow patterns. The results revealed that at the 0.14 m/s, bubbly, slug, and churn flow patterns were observed before the bend. While bubbly, stratified-wavy, and semi-annular flow was observed after the bend at Usg values of 0.05, 0.54, and 2.36 m/s, respectively. The results also presented the bubbly, slug, and churn flow patterns at Usl value of 0.38 m/s before the bend and compared with that flow patterns which were bubbly, slug, and semi-annular after the bend.

Musa et al [14] studied the flow patterns of the air-water two-phase flow in a vertical bend connected with a horizontal pipe with an internal diameter of 67 mm. The different operating ranges for water superficial velocities of 0.052 and 0.262 m/s with different range of air superficial velocities were used. The study reported that the bubbly flow pattern of the vertical flow altered to a stratified-wavy flow pattern at low values of Usl. The results also reported that the bubbly flow of the vertical flow changed to a plug pattern at a high rate of water flow rates in the horizontal flow lines. While the flow pattern becomes slug in the vertical pipe and altered to the stratified-wavy flow pattern at low values of Usl, and

then changed to slug flow pattern when the value of Usl increased. The churn flow pattern in the vertical flow lines changed to the stratified-wavy flow, and then changed to a semi-annular flow pattern at low values of Usl in the horizontal flow lines and then change to a wavy-annular flow regime when the values ofUsl increased. Different techniques have been used recently to classify the two-phase flow patterns in a blend such as Electrical Capacitance Tomography (ECT) as reported by Hampel et al. [15], X-ray tomography as presented by Abdulkareem et al. [16], and Wire-Mesh Sensor (WMS) as discussed by Rasteiro et al. [17] and Silva et al. [18].

As can be seen, there are much attention and many studies that are performed to investigate the two-phase flow patterns in a vertical, bend, and/or horizontal pipe. However, there is a lack of information on the two-phase flow behavior and bend effects on the two-phase flow patterns, which still need more investigation. This study presents an experimental investigation of air-water two-phase flow using a special geometry consists of a vertical pipe connected with a bend to change the flow direction to the horizontal. Different operating conditions for the air and water phases were used to cover the wide range of the two-phase flow patterns. Wire mesh sensor and Probability density function (PDF) were used to capture the two-phase flow patterns.

**Theory of Two-Phase Flow**

In the two-phase flow, the void fraction is the most important parameter that can be used to describe the behavior and development of the two-phase flow in a fluid domain. Many studies reported that the void fraction is a ratio of the gas velocity to the total velocity, which the liquid plus the gas velocity [18]. Equation 1 presents the void fraction as a function of gas and liquid velocity.

$$\alpha = \frac{Vgas}{Vliq+Vgas} \tag{1}$$

where the Vgas is the gas velocity and Vliq is the liquid velocity in the two-phase flow. There are many of the dimensionless parameters that can be used to present and define the two-phase flow patterns. Dean [3], Gardner and Neller [4] present some empirical correlations that can be used to estimate the Dean number (Dn) and Froude number (Fr) as follow,

$$Dn = Re(Dpipe/Rcurv)^2 \tag{2}$$

$$Fr = J^2/g \sin\theta \, Rcurv \tag{3}$$

Some other studies such as Usui et al. [6] presented the Froude number parameter for the two-phase flow patterns, which can be estimated as follows,

$$Fr = \frac{\rho_{liq}U_{sl}^2}{(\rho_{liq}-\rho_{gas})R_{curv}g(1-\varepsilon_{sg})^2}\left[1-\frac{\rho_{gas}}{\rho_{liq}}\left(\frac{U_{sg}(1-\varepsilon_{sg})}{U_{sl}\varepsilon_{sg}}\right)^2\right] \tag{4}$$

where: Re: Reynold number, Dpipe: Pipe diameter (m), Rcurv: Radius curvature of the bend (m), J: Phase velocity (m/s), $\theta$: Angular position, $\rho$liq: Density of the liquid (kg/m$^3$), $\rho$gas: Density of the gas (kg/m$^3$), Usl: Superficial velocity of the liquid (m/s), Usg: Superficial velocity of the gas (m/s), and $\boldsymbol{\varepsilon_{sg}}$: Straight pipe value.

The result can rely on the impact of system pressure. Thus, the pressure magnitude was measured by a gauge pressure (BUDENBERG, 0- 10546 kg/m$^2$) located after the gas rotometer. An empirical correlation to obtain the actual superficial velocity of air as shown in Equation 5 was used in the current experiment, which was utilized also by many studies such as Abdulkareem [24].

$$U_{actu.sg} = Q\sqrt{p}/A_p \tag{5}$$

Where (Uactu.sg) is the actual gas superficial velocity (m/s), Q is the volumetric flow rate (m$^3$/s), p is the absolute pressure at the gas rotameter flow rate (bar), and Ap is inside pipe area (m$^2$).

The PDF is a statistical tool utilized to distinguish flow design. If we designate a function p(x)dx in which the information x(t) is located between (x+dx) and x, so we will have:

$$p(x)\,dx = p(x < x(t) \le x + dx). \tag{6}$$

All the collected area related by this function should be with an equivalent unit,

$$p(-\infty < (x)\infty) = \int_{-\infty}^{+\infty} p(x)\,dx = 1. \tag{7}$$

For the void fraction, the PDF can be named as the rate of probability progress in that void faction exists in a specific range with void fractions.

The superficial velocity of fluid means the artificial velocity estimated by considering the given phase only one flowing in its cross-sectional area. While the inlet superficial velocity of any phase in this study denoted to the fluid velocity at rotameter measuring.

## 2. Materials and methods
### Experimental Setup and Calibration
A special experimental apparatus was designed and built to investigate the two-phase flow pattern through three combined components: transparent acrylic vertical and horizontal pipes of internal diameter 67 mm and outer diameter 72 mm, the acrylic 90-degree elbow of an internal diameter 67 mm and its curvature radius is 153.5 mm. Figure 1 illustrated the test section with the main components such as the air compressor, water tank, separator, and others. The 90-degree bend connected the vertical pipe with the horizontal pipe.

The utilized pipes with the 90-degree elbow were manufactured from transparent acrylic smooth material, so the friction produced from the wall of the inside pipe during the flow was neglected in the present test. A large water storage tank was used to keep the room temperature (22 C$^0$) unchanged to reduced uncertainty caused by the fluctuation of temperature degree. For the horizontal and vertical flow lines in large pipe diameters, gravitational and bouncy forces have the dominant influence on flow patterns, so other parameters were ignored.

The flow starts to enter the vertical pipe (downstream) then flows through the elbow 90-degree to change the flow direction to the horizontal (upstream). Air and water were supplied from the air compressor and water pump. The length of the vertical pipe is 6 m. The air-water enter the horizontal pipe which has the same diameter of that with the vertical and elbows 90-degree. Then the upstream of the air-water flow leaves the horizontal pipe at the atmospheric pressure. The test section consists of a vertical pipe connected with a 90-degree elbow then the outlet of the elbow was connected with the horizontal pipe as shown in Figure 2.

A range of operating conditions was used to perform the investigation of the two-phase flow patterns of the air-water flow in the experimental apparatus. Serice of experiments was conducted to cover 26 tests. The first 13 test had performed with changed the range of air superficial velocity (Usg) from 0.062 to 4.7 m/s for the specific water superficial velocity (Usl) of 0.157, while the second 13 test adapted the same ranges of Usg rates at the specific range of Usl of 0.314 m/s. Two WMS sensors were placed at two positions of the test section: at the entry of the elbow (exit of the vertical pipe), and at the exit of the elbow (entry to horizontal pipe) as shown in Figure 2 which presents the WMS with flanges that used in the connection.

Two of wire mesh sensors (WMS) with 24 X 24 wire mesh arrangement were used to measure the cross-section void fraction and its distribution in experiments and obtain a tomographic image for the two-phase flow pattern, as shown in Figure 3.
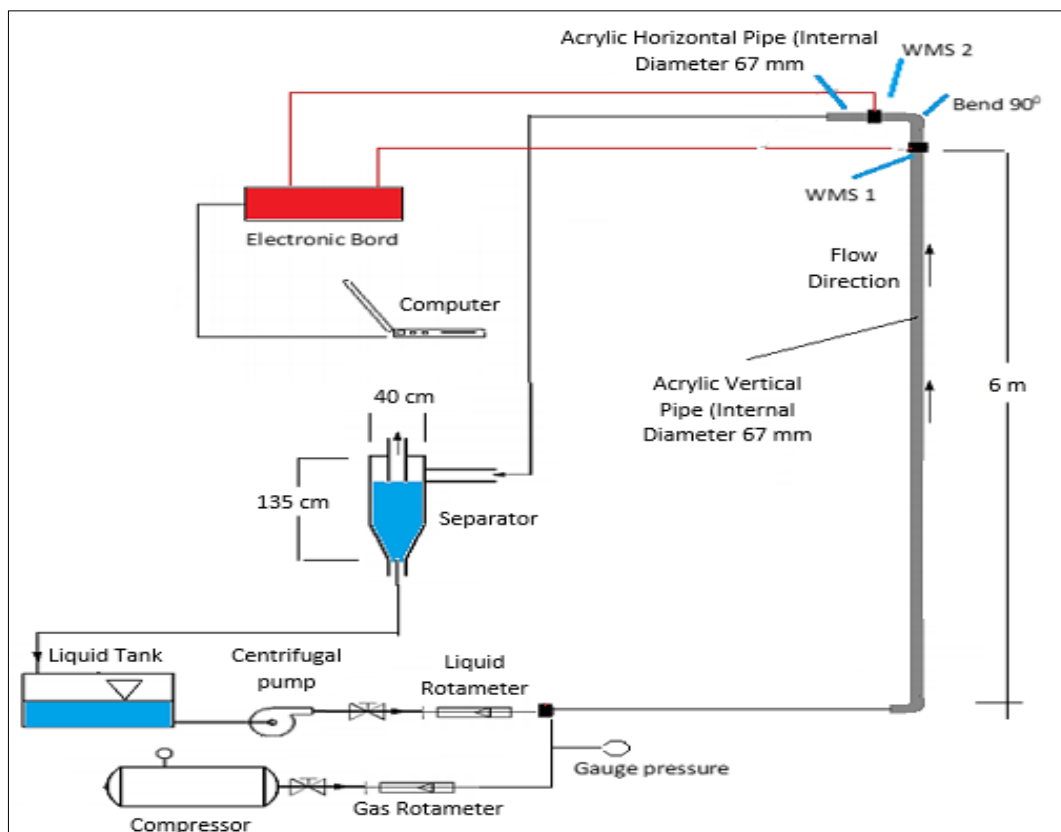
**Figure 1.** Experimental apparatus and the test section
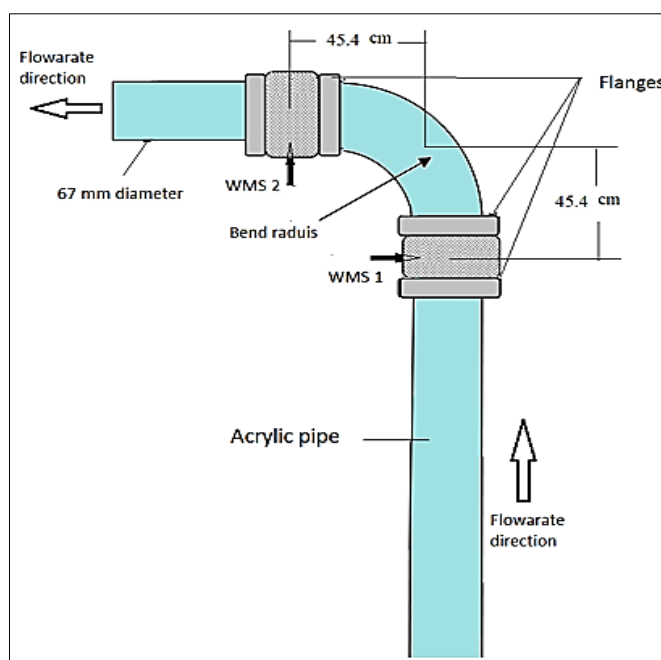


**Figure 2.** Test section with 90-degree to change the
flow from vertical to horizontal

The technique of using WMS is based on the ratio of (r/R) which represents the local radius (r) divided by the total radius of the pipe (R). The WMS was used in this work as a tomographic image sensor by utilizing the different electrical permittivity between air and water to estimate the void fractions ($\alpha$). At the cross-sectional area using the frequency of 1000 Hz to generate simultaneously tomography images by a special program called (CapWMS-display). Using WMS technology to measure the void fraction is

an effective way to obtain real data for the two-phase flow patterns, many studies were confirmed that such as the study conducted by Velasco Pena and Rodriguez [21].
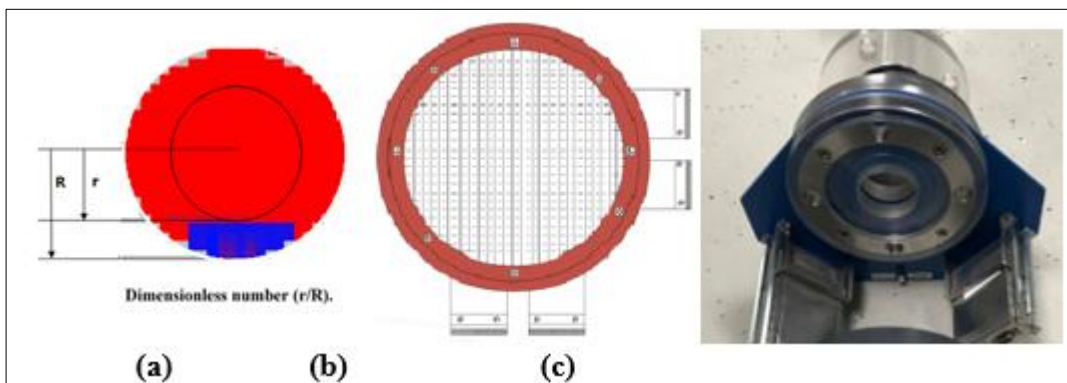


**Figure 3.** Wire mesh sensor: (a) cross-section void fraction distribution (the blue color is liquid and the red color is gas), (b) 24 X 24 mesh arrangement, and (c) the real WMS

In the experiments, measurements for the main parameters such as mass flow rate and pressure were measured. The temperature of the flow and pipe was assumed constant and there was nor the energy of heat source or added. The superficial velocity of the gas (Usg) in the horizontal pipe was fixed at certain value using equation 4.

The actual value of (Usg) was corrected by utilizing Equation 5 and the recorded pressure values as shown in Tables 1 and 2, as a result, the actual superficial velocities of air values are presented in Figure 4 and Figure 5.

**Table 1**. the correlations of Usg with pressure at Usl of 0.157 m/s

| Corrected Usg m/s | Pressure kPa | Inlet Usg m/s | |
|---|---|---|---|
| 0.0490 | 7.5842 | 0.05 | Run 1 |
| 0.0637 | 7.5842 | 0.062 | Run 2 |
| 0.2989 | 7.5842 | 0.28 | Run 3 |
| 0.3596 | 9.3079 | 0.34 | Run 4 |
| 0.4227 | 9.3079 | 0.4 | Run 5 |
| 0.5680 | 9.3079 | 0.5 | Run 6 |
| 0.7409 | 9.3079 | 0.7 | Run 7 |
| 0.9909 | 9.9974 | 0.9 | Run 8 |
| 1.4956 | 11.3763 | 1.4 | Run 9 |
| 2.0002 | 12.0658 | 1.9 | Run 10 |
| 2.5117 | 13.1000 | 2.36 | Run 11 |
| 3.0231 | 13.7895 | 2.83 | Run 12 |
| 5.2600 | 24.1316 | 4.7 | Run 13 |

**Table 2**. the correlations of Usg with pressure
at Usl of 0.314 m/s

| Corrected Usg m/s | Pressure kPa | Inlet Usg m/s | |
|---|---|---|---|
| 0.0490 | 7.58423 | 0.05 | Run 1 |
| 0.0637 | 7.5842 | 0.062 | Run 2 |
| 0.2989 | 7.5842 | 0.28 | Run 3 |
| 0.3568 | 7.5842 | 0.34 | Run 4 |
| 0.4193 | 7.5842 | 0.4 | Run 5 |
| 0.5680 | 9.3079 | 0.5 | Run 6 |
| 0.7443 | 10.342 | 0.7 | Run 7 |
| 0.9940 | 10.686 | 0.9 | Run 8 |
| 1.5115 | 13.789 | 1.4 | Run 9 |
| 2.021 | 14.479 | 1.9 | Run 10 |
| 2.5641 | 17.926 | 2.36 | Run 11 |
| 3.1211 | 21.373 | 2.83 | Run 12 |
| 5.4306 | 32.405 | 4.7 | Run 13 |
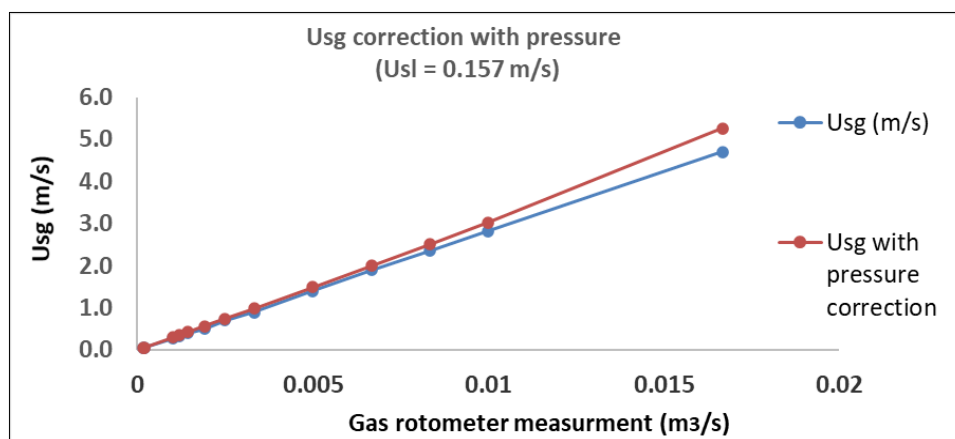


**Figure 4.** The correction between the inlet and actual (Usg) with pressure
at constant (Usl) value of 0.157 m/s
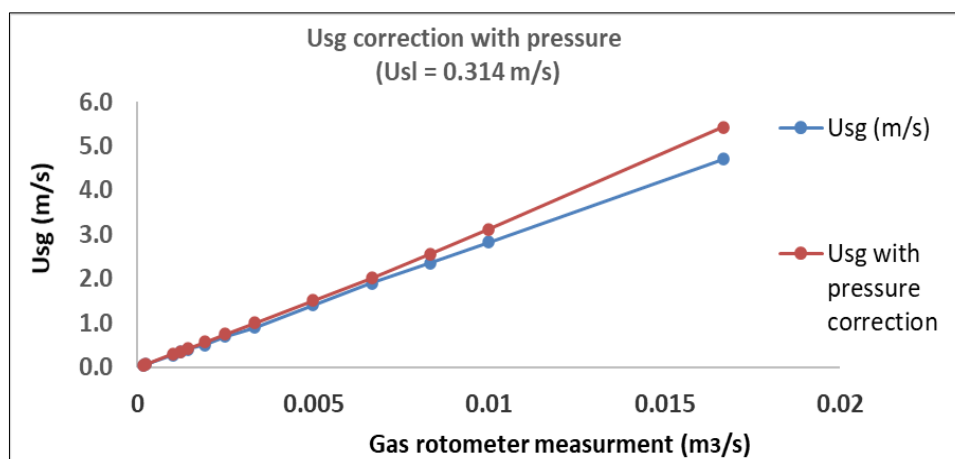
**Figure 5.** The correction between the inlet and actual (Usg) with pressure
at constant (Usl) value of 0.314 m/s

## 3. Results amd discussions

A series of experiments have been completed to investigate the two-phase flow patterns and record about 60000 samples for the void fraction for each operating condition. The results were collected using the wire mesh sensors at certain operating conditions for the air and water superficial velocities. MATLAB and a special virtual basic code were used to analyze and present the data and result. Image tomographic technique was also used to analyze the two-phase flow patterns, so void fraction, probability density function (PDF) for the presented test section, and the specific operating conditions would be discussed and presented in this section.

### 4.1. Tomographic Images

Figures 6 and 7 presented the tomographic images before and after the bend for different values of the gas superficial velocity at a constant liquid superficial velocity of 0.157 and 0.314 m/s. Two of WMS with 24 X 24 mesh arrangement were used to capture data for each run and to present the flow distribution and its behavior in the vertical and horizontal pipe (before and after the bend). Two-phase flow in pipes is nonhomogeneous flow and it is an unpredictable flow, and its pattern is changed frequently in a low limit, thus the considerations of capturing more than one image of each run are more acceptable to identify which pattern is more applicable of every case. Therefore, 6 cross-sectional tomographic images of the vertical and horizontal flowlines are captured for each run as one image for every 10 seconds, the total period for one run was 60 seconds. As can be seen from Figure 6, the two-phase flow patterns at the inlet of bend were changed from bubbly at Usg of 0.064 m/s, slug at Usg from 0.299 to 0.991 m/s, and then churn flow from 2.521 to 3.023 m/s at constant Usl of 0.157 m/s.

In contrast, the flow patterns at the outlet of the bend where the flow becomes horizontal and using the same operating conditions the patterns were observed as stratified-wavy at Usg range from 0.064 to 2 m/s, wavy annular at Usg range from 0.299 to 3.023 m/s, and then semi-annular at Usg of 5.26 m/s.

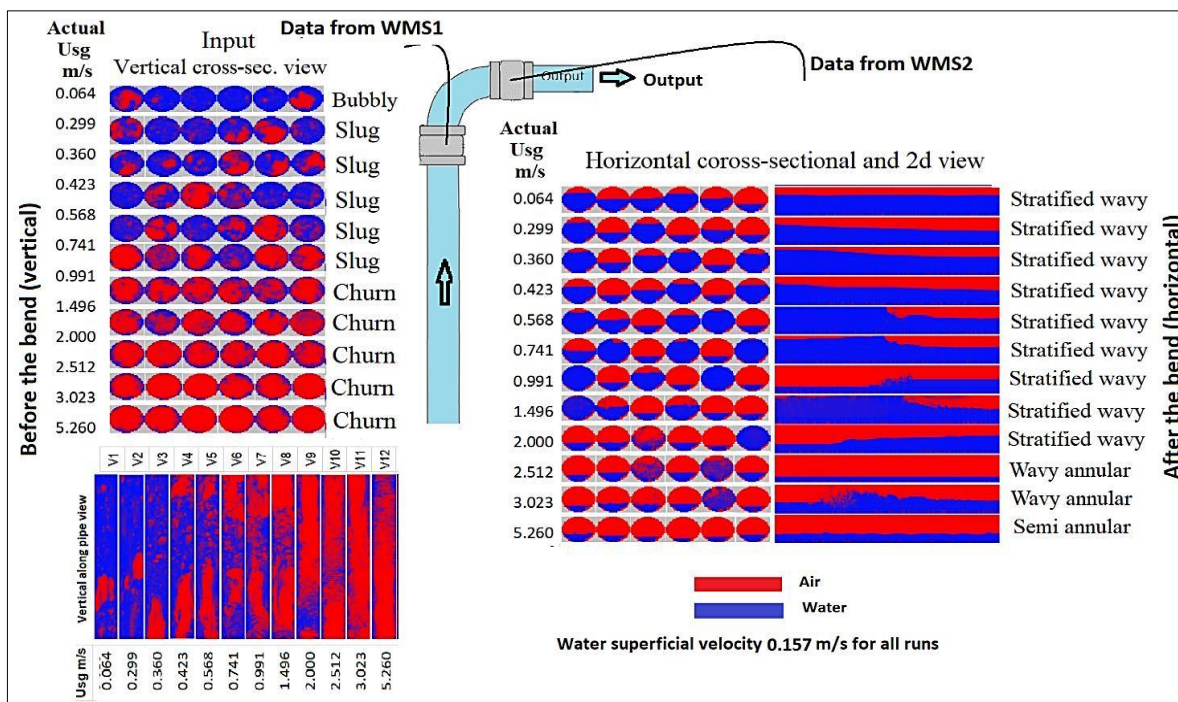**Figure 6.** Tomographic images before and after at different Usg values with a constant Usl value of 0.157 m/s

Figure 7 presents the tomographic images before and after the bend for different values of the gas superficial velocity at a constant liquid superficial velocity of 0.314 m/s. The flow patterns in the developed vertical flow line were observed to be bubbly at Usg 0.064 m/s, slug flow from 0.299 to 0.996 m/s, and churn flow from 1.525 to 5.596 m/s. Meanwhile, at the bend inlet in the horizontal flow lines, the flow regimes were observed as bubbly flow at Usg value of 0.064 m/s, plug flow at 0.299 m/s, slug flow from 0.357 to 0.996 m/s, stratified wavy flow from 1.525 to 3.165 m/s and wavy annular flow at Usg value of 5.596 m/s
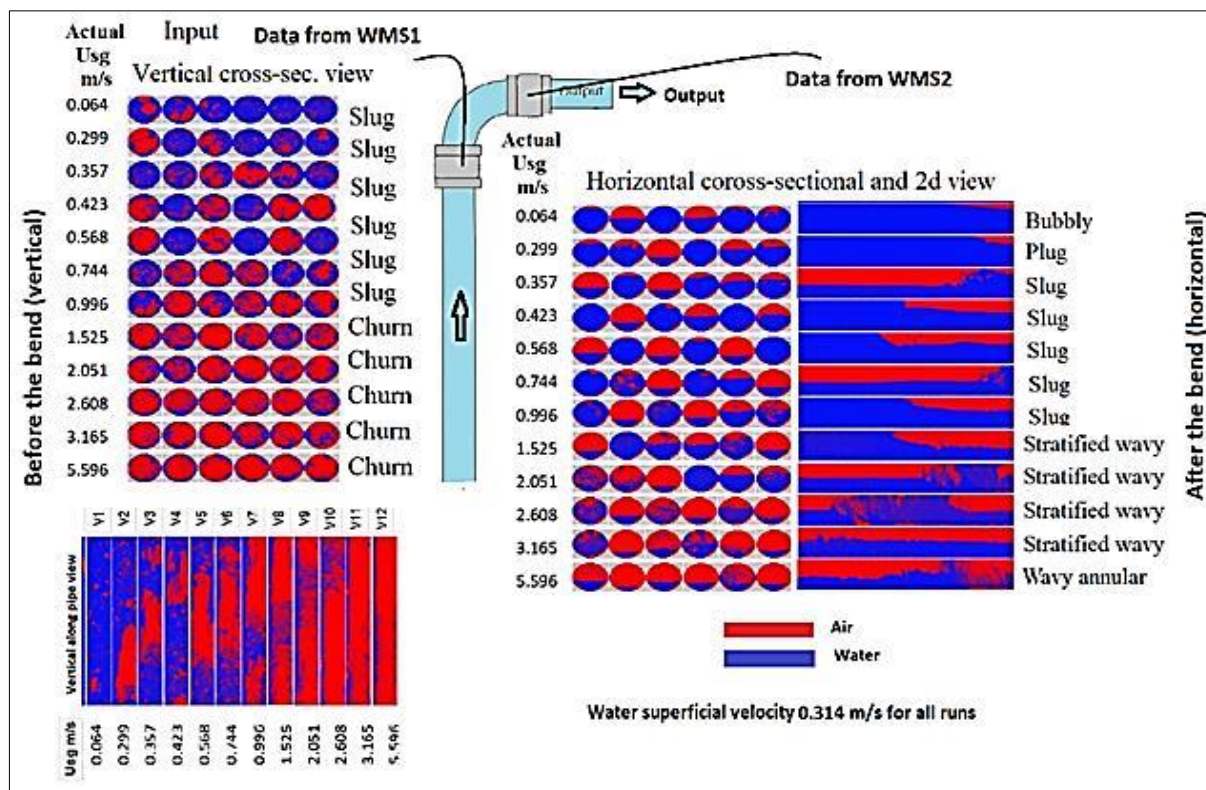
**Figure 7.** Tomographic images before and after at different Usg values with a constant Usl value of 0.314 m/s

## 4.2. Probability Density Function (PDF) Analysis

Figure 8 presents the probability density function (PDF) when the Usl equal to 0.157 m/s and actual Usg change from 0.064 m/s to the 5.26 m/s through the vertical and horizontal pipe crossing the 90-degree bend. The void fraction was presented in Figure 8 in orange and blue lines to capture the two-phase flow pattern at the inlet and outlet of the bend. So, the PDF technique can capture the flow patterns based on the number and peaks behavior. As can be seen from Figure 8 the recorded signal represents the bubbly two-phase flow pattern at the inlet of the bend. In contrast, the curve of PDF was recorded at 0.15 which gave the range of void fraction from 0.3 to 0.55 at the outlet of the bed, the stratified-wavy flow pattern was recorded and observed. The two-phase flow pattern was changed and affected by the bend and as a result of turbulent behavior inside the bend, the two-phase flow pattern can not be stable and keep the same flow pattern between the inlet and outlet of the bend.

When the Usg increased to 0.299 m/s, the PDF recorded two peaks at 0.01 and 0.05 for the vertical flow inside the vertical pipe. The increasing of Usg increase the Taylor bubbles length also to produce a slug flow pattern. At the outlet of the bend and flow direction change, the flow pattern was observed as a stratified-wavy flow pattern as a result of the bend which influenced the flow pattern. The PDF was recorded as multiple peaks at 0.4. In the horizontal, the flow behavior was observed as a wavy flow pattern.
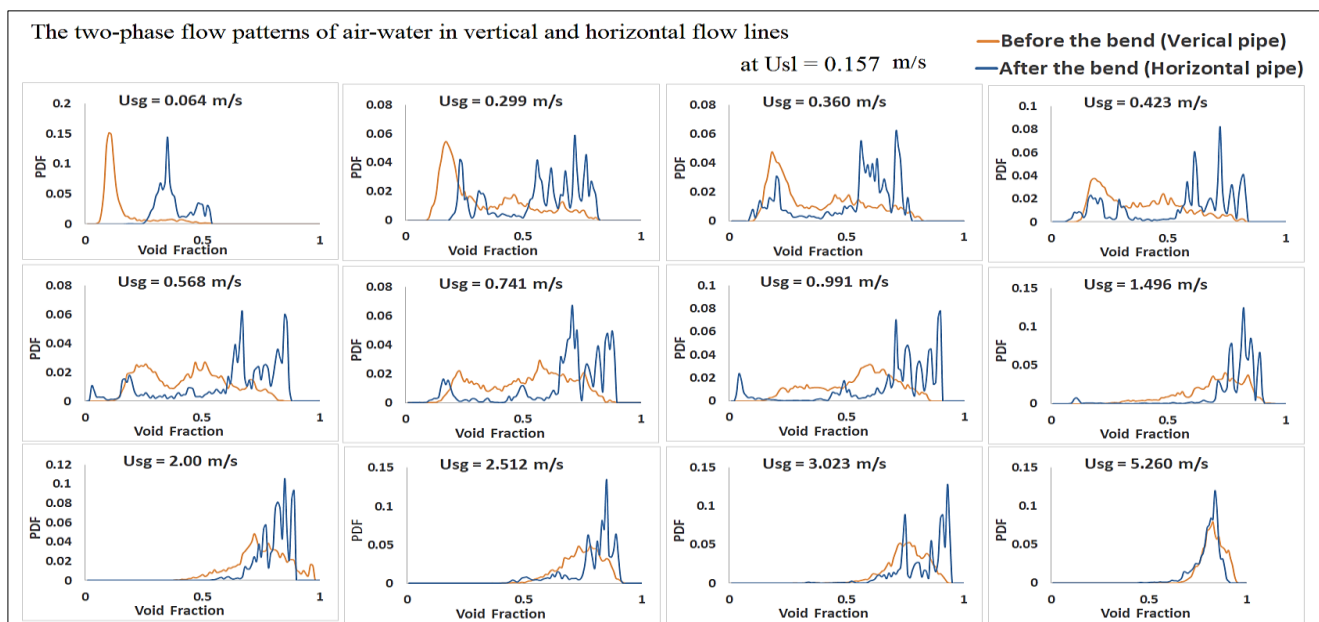
**Figure 8.** Probability Density Function (PDF) at Usl value of 0.157 m/s

When the Usg increased further to 1.496 m/s, the flow pattern is completely developed to churn pattern at the inlet of the bend. While the flow pattern at the outlet of the bend was recorded as a stratified-wavy flow pattern at the same value of Usg. By increasing the Usg to 2.512 m/s, the flow pattern at the inlet and outlet of the bend developed to churn and wavy annular respectively. At the maximum gas superficial velocity Usg of 5.26 m/s, the two-phase flow pattern at the outlet of the bend was a semi-annular flow pattern and in the vertical pipe and at the inlet of the bend the flow pattern was churn. The PDF presents the two-phase flow pattern at Usg of 5.26 m/s as one peak but the peak was shifted to the right side compared with that when the Usg equal to 0.064 m/s.
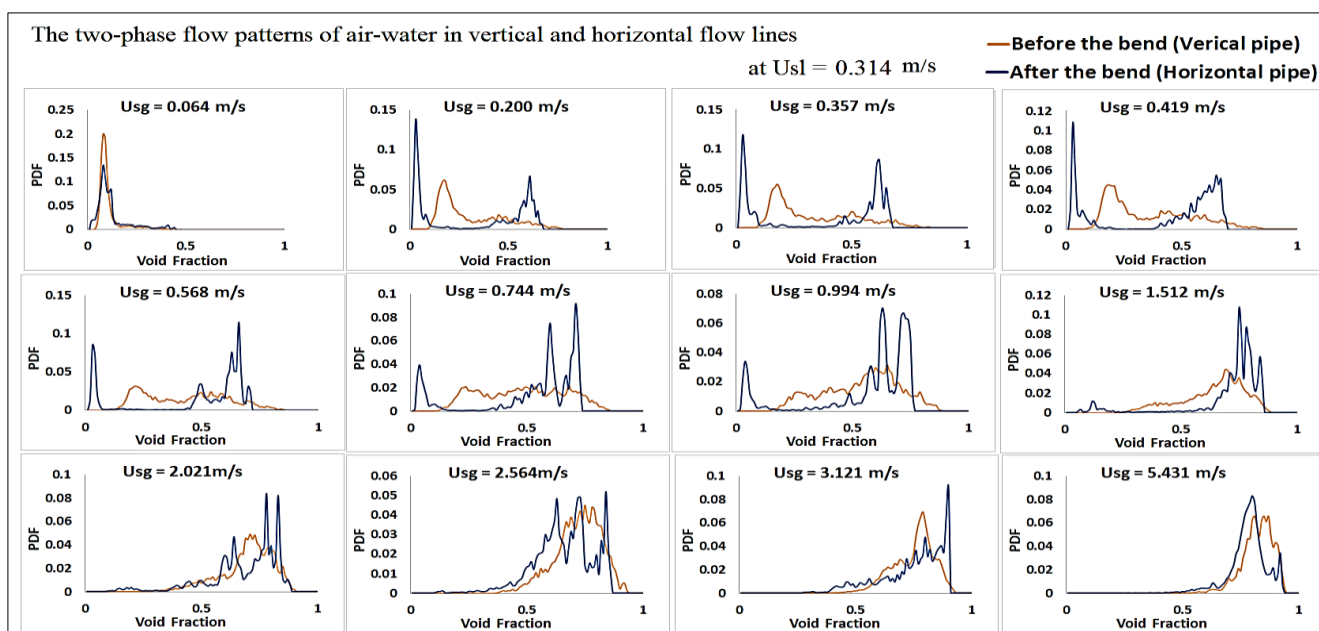


**Figure 9.** Probability Density Function (PDF) at Usl value of 0.314 m/s

Figure 9 presents the PDF results for the two-phase flow patterns at liquid superficial velocity Usl of 0.314 m/s. As can be seen from Figure 8 when the gas superficial velocity Usg change from 0.064 to

5.431 m/s, the PDF plot change as the two-phase flow pattern change based on the Usg. When Usg equal to 0.064 m/s, the flow pattern was observed and captured by PDF as a bubbly flow pattern in both of vertical and horizontal lines. The range of void fraction was captured between 0.1 to 0.5 and the peak is shifted to the left. Stratifiedwavy flow pattern was recorded when the Usg covered the range from 1.512 to 3.121 m/s and wavy-annular flow pattern in the horizontal flow pipe when the Usg was equal to 5.431 m/s.

## 4.3 Two-Phase Flow pattern Map

The two-phase flow pattern map was created and compared with that of Taitel et al. [5]. Figure 10 presents the two-phase flow pattern for the vertical flow of the test section which represents the inlet flow to the bend. Figure 10 presents the bubbly, plug, slug, and churn two-phase flow pattern which was observed in the vertical pipe at various liquid and gas superficial velocities. It is clear that the gas superficial velocity has a significant effect on the flow pattern when the liquid superficial velocity remains constant. The two-phase flow pattern map gives good agreement with the map presented by Taitel et al. [5].
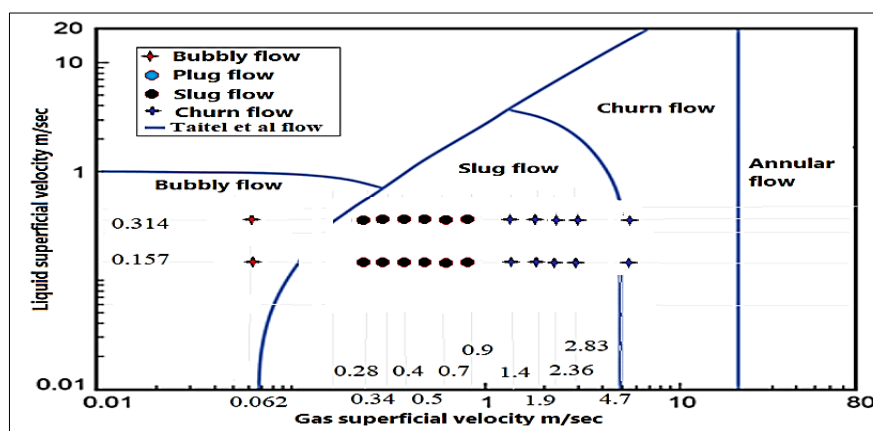


**Figure 10.** Two-phase flow patterns map for the vertical pipe of the test section

Figure 11 presents the two-phase flow pattern for the horizontal flow of the test section which represents the outlet of the bend. The Figure presents the stratified-wavy, bubbly, plug, slug, wavy-annular, and semi-annular two-phase flow patterns which were observed in the horizontal part of the test section at various liquid and gas superficial velocities. The gas superficial velocity has a significant effect on the flow pattern when the liquid superficial velocity remains constant. The two-phase flow pattern map gives good agreement compared with the two-phase flow pattern map presented by Mandhane et al [22].
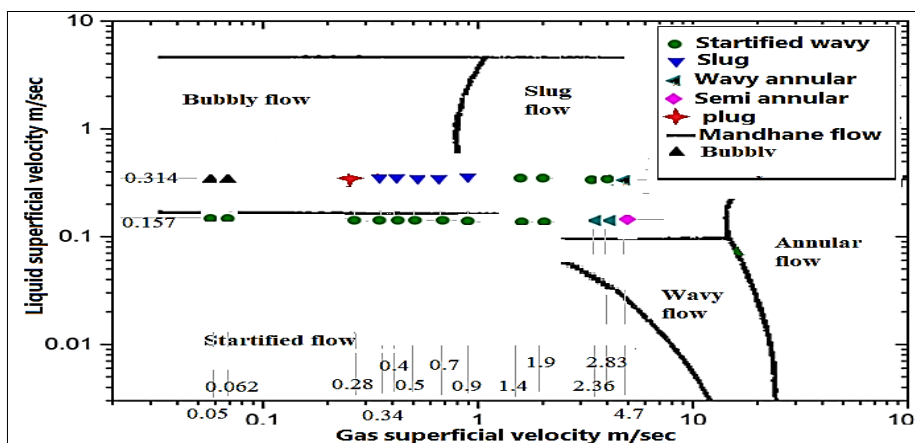


**Figure 11.** Two-phase flow patterns map for the horizontal
pipe of the test section

### 4.4 Mean Void Fraction Distribution Regarding Pipe Diameter

The current test was conducted 26 runs, where every run was performed at constant superficial velocities of the air and water for 60 seconds by using two WMS (frequency of 1000 frames/s) to obtain 60000 values of void fractions. The mean void fraction of every run is representing the average value of 60000 readings. Figures 12 and 13 present the mean void fraction distribution for both vertical and horizontal pipes when the Usl is 0.157 and 0.314 m/s respectively. In Figure 12 (a) the mean of cross-section void fraction of the vertical pipe decreased linearly when the ration of (r/R) increased, the bubbly two-phase flow pattern was captured and observed. The bubbles concentrate in the center of flow due to the surface tension and gravity that effected between the water and the wall of the pipe. Churn, and slug two-phase flow patterns were observed when the Usg increased from 0.299 to 5.26 m/s because bubbles started to coalescence in the middle of the pipe. A similar trend was obtained in Figure 13 (a) for the vertical pipe when the Usl increased to 0.314 m/s.

When the Usg value is equal to 0.064 m/s, the horizontal pipe is filled with water at the centerline axis that slightly increased the mean void fraction (α) with the increased value of (r/R) as shown in Figure 12 (b). However, when the (r/R) decreased and the Usg is 0.314 m/s the void fraction increased which means there are more bubbles of air in the horizontal pipe, Figure 13 (b). In the horizontal pipe, the distribution of the mean void fraction (α) covered semi-annular, wavy annular, and the stratified wavy regime. The α decreased with increasing the ratio of (r/R). For the bubbly flow patterns, α was slightly increased with increasing of (r/R).
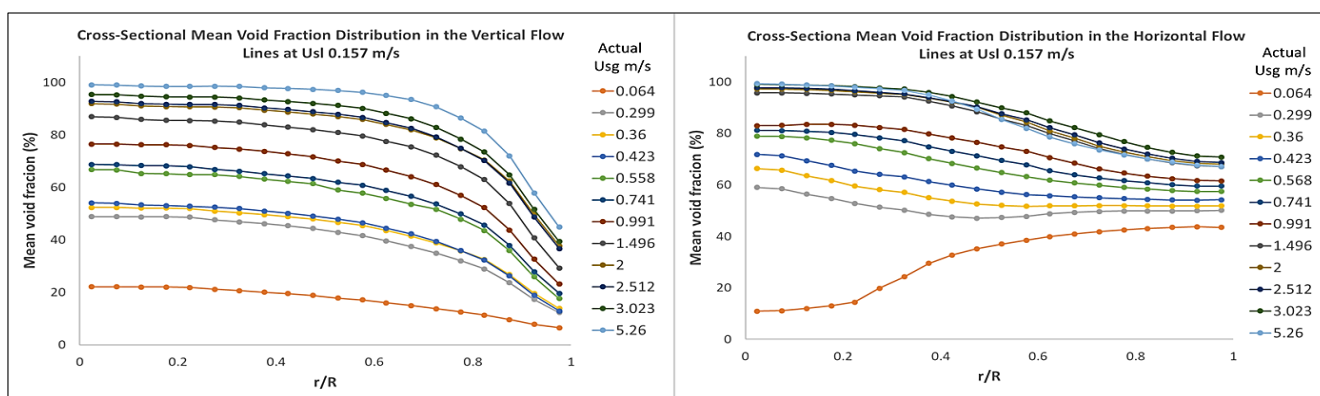


**(a)**                                                          **(b)**

**Figure 12.** The cross-sectional mean void fraction distribution at various (r/R) and Usl of 0.157 m/s; (a) void fraction for the vertical pipe, (b) void fraction for the horizontal pipe.
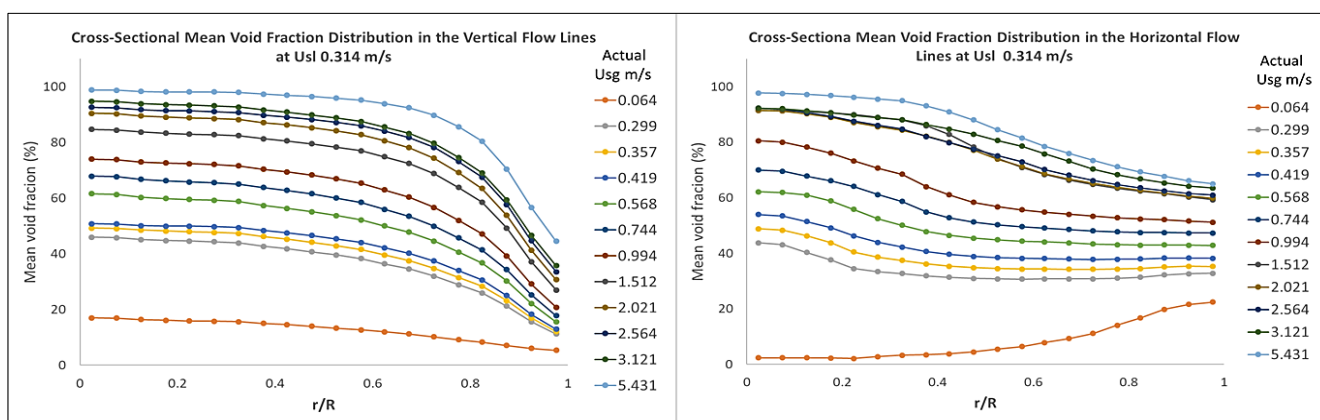


**(a)**                                                          **(b)**

**Figure 13.** The cross-sectional mean void fraction distribution at various (r/R) and Usl of 0.314 m/s; (a) void fraction for the vertical pipe, (b) void fraction for the horizontal pipe

# 4. Conclusions

The cross-sectional void fractions of the vertical and horizontal pipes with the constructed tomographic images have been estimated by utilizing two WMS sensors. The required data have been used to study the elbow effect and to distinguish the flow patterns in both pipes by analyzing the Probability Density Function (PDF), flow regime maps, and the mean void fraction distribution regarding pipe diameter. The present study has summarized the following:

- The increased value of the superficial velocity of water (Usl) from 0.157 to 0.314 m/s has no significant effect on the flow patterns of the vertical flow lines, where the flow patterns have been observed in the vertical section as a bubbly flow when the Usg value was 0.064 m/s, slug flow when the Usg value was in the range from 0.299 to 0.991 m/s and finally churn flow when the Usg value was in the range from 1.496 to 5.26 m/s.

- At the constant value of liquid superficial velocity Usl 0.157 m/s, the flow patterns were observed as stratified-wavy when the Usg value was in the range from 0.064 to 2 m/s, wavy annular when the Usg value was in the range from 2.521 to 3.023 m/s, and finally, a semi-annular flow when Usg value was 5.26 m/s.

- At the constant value of Usl 0.314 m/s, the flow patterns in the horizontal pipe were observed as bubbly flow when the Usg value was 0.064 m/s, plug flow when the Usg value was 0.299 m/s, slug flow when the Usg value was in the range from 0.357 to 0.996 m/s, stratified wavy flow when the U sg was changed from 1.525 to 3.165 m/s, and finally wavy annular flow pattern when the Usg value was 5.596 m/s.

- The significant impact of the gravitation force and the buoyancy force on the horizontal flow lines regime are observed. These forces acted on the flow and forced the water phase to flow inside the region of the bend centerline while the air phase flows at the outside region of the bend centerline. As a result, the coalescence bubbles will be broken up in the bend entrances during the imbalance which occurred by the surface tension and the centrifugal force, the flow patterns at the bend outlet may show a different behavior rather than developed horizontal flow in pipes.

- The slug and plug flow patterns impacted the fatigue and dynamic stress of the piping systems, and both patterns rise the pressure oscillations in pipes, besides that is led to affect the physical properties of the pipes and bends. Thus, under the current test condition should avoid the superficial velocities of air and water that caused those patterns.

- The analysis of PDF is a more reasonable technique to identify the two-phase flow pattern of vertical flow lines, but the classification of two-phase flow patterns in the horizontal flow line is more sophisticated and requires more than one method besides the PDF method like tomographic images.

**References**
1. AZZI, A., BELAADI, S., AND FRIEDEL, L., Two-phase gas/liquid flow pressure loss in bends, Forsch. im Ingenieurwes., **65**(10), 2000, 309-318.
 https://link.springer.com/article/10.1007/s100100000030.
2. ITO, H., Flow in curved pipes, Biosci. Biotechnol. Biochem., **33**(4), 1985, 1660-1668.
https://doi.org/10.1299/jsme1987.30.543.
3. DEAN, W. R., Note on the motion of fluid in a curved pipe," Dublin Philos. Mag. J. Sci., **4**(20), 1927, 208-223.
https://www.tandfonline.com/doi/abs/10.1080/14786440708564324.
4. GARDNER, G. C. and NELLER, P. H., Phase distributions in flow of an air-water mixture round bends and past obstructions at the wall of a 76-mm bore tube, Proc. Inst. Mech. Eng., **184**(33), 1969, 36.

https://journals.sagepub.com/doi/abs/10.1243/PIME_CONF_1969_184_084_02.

5. TAITEL, Y. and DUKLER, A. E., A model for predicting flow regime transitions in horizontal and near horizontal gas-liquid flow, AIChE J., **22**(1), 1976, 47-55.
https://aiche.onlinelibrary.wiley.com/doi/abs/10.1002/aic.690220105.

6. USUI, K., AOKI, S., and INOUE, A., Flow behavior and phase distribution in two-phase flow around inverted u-bend, J. Nucl. Sci. Technol., **20**(11), 1983, 915-928.
https://doi.org/10.1080/18811248.1983.9733489.

7. KIM, S., PARK, J. H., KOJASOY, G., KELLY, J. M., and MARSHALL, S. O., Geometric effects of 90-degree elbow in the development of interfacial structures in horizontal bubbly flow, Nucl. Eng. Des., **237**, (20-21), 2007, 2105-2113.
https://doi.org/10.1016/j.nucengdes.2007.02.007.

8. ABDULKADIR, M., ZHAO, D., SHARAF, S., ABDULKAREEM, L., LOWNDES, I. S., and AZZOPARDI, B. J., Interrogating the effect of 90° bends on air-silicone oil flows using advanced instrumentation," Chem. Eng. Sci., **66**(11), 2011, 2453-2467.
https://doi.org/10.1016/j.ces.2011.03.006.

9. DE SALVE, M., MONNI, G., and PANELLA, B., Horizontal air-water flow analysis with wire mesh sensor, in 6th European Thermal Sciences Conference (Eurotherm 2012), 2012, 0-8.
https://iopscience.iop.org/article/10.1088/1742-6596/395/1/012179/pdf.

10. LIU, W., TAN, C., and DONG, F., Local characteristic of horizontal air-water two-phase flow by wire-mesh sensor, Trans. Inst. Meas. Control, **92**, 2016, 1-16.
https://doi.org/10.1177/0142331216665689.

11. KONG, R., RAU, A., LU, C., GAMBER, J., and KIM, S., Experimental study of interfacial structure of horizontal air-water two-phase flow in a 101.6 mm ID pipe, Exp. Therm. Fluid Sci., **93**, 2018, 57-72.
https://doi.org/10.1016/j.expthermflusci.2017.12.016.

12. BRESSANI, M. and MAZZA, R. A., Two-phase slug flow through an upward vertical to horizontal transition, Exp. Therm. Fluid Sci., **91**, 2018, 245-255.
https://doi.org/10.1016/j.expthermflusci.2017.10.023.

13. ABDULKADIR, M., Experimental and computational fluid dynamics (CFD) studies of gas-liquid flow in bends, PhD. thesis, University of Nottingham, 2011.

14. MUSA, V. A., ABDULKAREEM, L. A., and ALI, O. M., Experimental Study of the Two-Phase Flow Patterns of Air-Water Mixture at Vertical Bend Inlet and Outlet, Eng. Technol. Appl. Sci. Res., **9**(5), 2019, 4649-4653.
https://www.etasr.com/index.php/ETASR/article/view/3022/pdf.

15. HAMPEL, U., SPECK, M., MENZ, H. J., SCHLEICHER, E., and PRASSER, H. M., Experimental ultra fast x-ray computed tomography with a linearly scanned electron beam source, Flow Meas. Instrum., **16**(2-3), 2005, 65-72.
https://doi.org/10.1016/j.flowmeasinst.2005.02.002.

16. ABDULKAREEM, L. A., ESCRIG, E., REINECKE, S., HEWAKANDAMBY, B. N., and AZZOPARDI, B. J., Tomographic interrogation of gas-liquid flows in inclined risers, in ICMF-2016 – 9th International Conference on Multiphase Flow, Firenze, Italy, 2016.

17. RASTEIRO, M. G., SILVA, R., GARCIA, F. A. P., and FAIA, P., Electrical tomography: a review of configurations and applications to particulate processes, KONA Powder Part. J., **29**(29), 2011, 67-80.
https://doi.org/10.14356/kona.2011010.

18. DA SILVA, M. J., THIELE, S., ABDULKAREEM, L. AZZOPARDI, B. J., and HAMPEL, U., High-resolution gas-oil two-phase flow visualization with a capacitance wire-mesh sensor, Flow Meas. Instrum., **21**(3), 2010, 191-197.
https://doi.org/10.1016/j.flowmeasinst.2009.12.003.

19. PRASSER, H. M., BÖTTGER, A., and ZSCHAU, J., A new Electrode-Mesh Tomograph for Gas-Liquid Flows, Flow Meas. Instrum., **9**(2), 1998, 111-119.
https://doi.org/10.1016/S0955-5986(98)00015-6.

20. JOHNSON, I. D., Method and apparatus for measuring water in crude oil, no. 19. US Patent, 1987.
21. VELASCO PEÑA, H. F., RODRIGUEZ, O. M. H., Applications of wire-mesh sensors in multiphase flows, Flow Meas. Instrum., **45**, 2015, 255-273.
22. MANDHANE, J. M., GREGORY, G. A., and AZIZ, K., A flow pattern map for gas-liquid flow in horizontal pipes, Int. J. Multiph. Flow, **1**(4), 1974, 537-553.
https://doi.org/10.1016/0301-9322(74)90006-8.
23. KAJERO, O. T., AZZOPARDI, B. J., and ABDULKAREEM, L, Experimental study of viscous effects on flow pattern and bubble behavior in small diameter bubble column, Phys. Fluids, vol. **30**(9), 2018, 93101(1–16).
24. ABDULKAREEM, L. A., Tomographic investigation of gas-oil flow in inclined risers, PhD thesis, University of Nottingham, 2011, 127

Manuscript received: 31.08.2020